Secondary User Access Control in Cognitive Radio Networks

Huaxia Wang, *Student Member, IEEE*, Yu-Dong Yao, *Fellow, IEEE*, Xin Zhang, and Hongbin Li, *Senior Member, IEEE*

***Abstract*— Spectrum sharing and aggregation among authorized secondary users (A-SUs) are important tasks in operating effective cognitive radio networks. Furthermore, in protecting spectrum sharing/aggregation against unauthorized secondary users (UA-SUs), secondary user access control (SUAC) is needed, which is investigated in this paper. A jamming signal is injected to degrade the spectrum sensing performance of UA-SUs, while reliable spectrum sensing performance for A-SUs can be achieved through an oblique projection-based jamming cancellation method. An orthogonal frequency division multiplexing-based transmission model is considered in this paper. The generalized likelihood ratio test algorithm is used for both authorized and unauthorized SUs in spectrum sensing. Numerical results show the effectiveness of the proposed SUAC in degrading the spectrum sensing performance of the unauthorized SUs.**

***Index Terms*— Cognitive radio, jamming, OFDM, spectrum sensing, access control.**

I. Introduction

COGNITIVE radio (CR) technologies [1] have been extensively studied to improve the spectrum utilization. In CR networks, a spectrum band becomes available when primary users (PUs) are not active in that band and secondary users (SUs) are able to utilize the spectrum band or channel after performing spectrum sensing (i.e., identification of white space). Therefore, spectrum sensing is a critical step or task in CR [2], [3]. In [4], a generalized likelihood ratio test (GLRT) based spectrum sensing approach was presented. By using detection variables based on the eigen-decomposition of the sampling covariance matrix, an eigenvalue-based spectrum sensing algorithm for CR was presented in [5]. It is known that, with appropriate spectrum sensing algorithms, SUs are able to effectively utilize spectrum white space in CR networks.

However, due to the open and dynamic nature of CR networks, especially under spectrum sharing and aggregation [6], [7], there can be significant security vulnerabilities (e.g., primary user emulation (PUE) attack [8], most active band (MAB) attack [9], and spectrum sensing data falsification (SSDF) attack [10]). Notice that, in this paper, we focus on the issue of authorized secondary users (A-SUs) versus unauthorized secondary users (UA-SUs) in spectrum access. It is desirable for a spectrum owner or spectrum manager to perform secondary user access control (SUAC), in which A-SUs are permitted to utilize the spectrum white space while UA-SUs are not allowed to use the spectrum. SUAC can also be utilized when implementing resource management for spectrum pricing [11], [12], priority control, etc.

Recently, a coordinated jamming and communications (CJamCom) technique [13] was introduced to prevent enemy users' communications while maintain reliable communications performance for friendly users. Similarly, an SUAC method is introduced in this paper to disrupt UA-SUs' operation while achieve reliable spectrum sensing and transmission performance for A-SUs. Specifically, a jamming signal is injected by a PU, spectrum owner, or spectrum manager, to suppress UA-SUs' spectrum sensing capability. The jamming features can be obtained by A-SUs only. Thus the A-SUs can either suppress or eliminate the jamming signal when performing spectrum sensing, while UA-SUs will suffer significant sensing performance degradation due to the jamming signal.

In a related research topic, physical layer security in terms of information theoretic analysis has attracted considerable attention [14]–[19]. In [15], a transmitter ensures secret/reliable communications by producing an artificial noise to degrade an eavesdropper's channel. Reference [16] proposes secure communications for one source-destination pair through cooperative relays in the presence of multiple eavesdroppers. The relationship between CR and secrecy communications was presented in [17], in which an underlay transmission scenario was considered. Reference [17] shows that, under properly selected interference temperature constraints, the optimal transmit covariance to maximize the achievable CR spectrum sharing capacity is the same as the maximum secrecy rate. In addition, physical layer security based CR designs have been investigated recently [18].

This paper differs from the physical layer security based transmission model [14]–[17], which guarantees secure transmissions by exploiting the physical characteristics of the communication channel [16], while the proposed SUAC technique does not rely on any communication channel information in designing the secret jamming signal. Notice that this paper also differs from the CJamCom technique [13] which addresses multiuser transmission scenarios and SUAC is a single transmitter (PU) environment during spectrum sensing. In this paper, we consider an SUAC model in an orthogonal frequency division multiplexing (OFDM)

Manuscript received April 5, 2016; revised July 22, 2016 and September 27, 2016; accepted September 30, 2016. Date of publication October 5, 2016; date of current version November 3, 2016.

The authors are with the Department of Electrical and Computer Engineering, Stevens Institute of Technology, Hoboken, NJ 07030 USA (e-mail: hwang38@stevens.edu; yyao@stevens.edu; xzhang23@stevens.edu; Hongbin.Li@stevens.edu).

Color versions of one or more of the figures in this paper are available online at http://ieeexplore.ieee.org.

Digital Object Identifier 10.1109/JSAC.2016.2615262

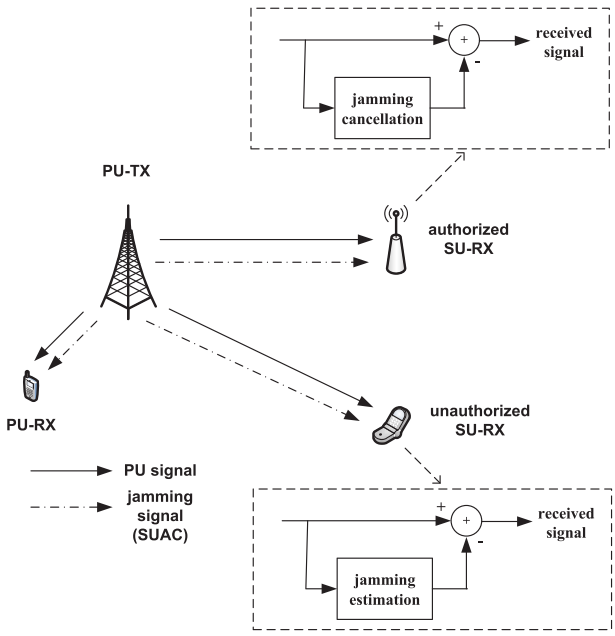

Fig. 1. Communications system model.

communication architecture [20]. At the transmission side (a PU, spectrum owner, or spectrum manager), a multitone jamming signal is generated and the jamming sequence features can only be obtained by A-SUs. At the receiving end, through the GLRT [21] technique and oblique projection [22], [23], A-SUs are able to achieve reliable spectrum sensing performance, while UA-SUs suffer significant sensing performance degradation.

The paper is organized as follows. In Section II, the SUAC architecture and communications model are presented. Section III presents the performance analysis of the GLRT detector for both authorized and unauthorized SUs. Section IV presents simulation results and related discussions. Finally, conclusions are given in Section V.

Notation: Matrices/vectors are denoted as boldface upper/lower letters; $(\cdot)^T$, $(\cdot)^H$, $(\cdot)^{-1}$ and $(\cdot)^\dagger$ represent transpose, conjugate transpose, inverse and pseudo-inverse, respectively; $*$ denotes Hadamard product and $\otimes$ is the Kronecker product; diag (d_i) denotes a diagonal matrix with i^{th} diagonal entry d_i. span $(\mathbf{A})$ represents the subspace spanned by the columns of matrix $\mathbf{A}$.

II. Secondary User Access Control and Communications System Model

A. Secondary User Access Control

The basic idea of the SUAC technique is illustrated in Fig. 1. We consider that there are two types of SUs, A-SUs and UA-SUs. At the transmission side, a spectrum owner or PU deliberately generates a jamming signal which will be transmitted together with the PU signal. At the receive end, since A-SUs have the knowledge of the jamming signal (e.g., jamming pattern), with oblique projection [24] or some other interference cancellation techniques, the jamming signal can be either eliminated or suppressed. However, for UA-SUs, even if they might know the existence of the jammer, it is still difficult to eliminate or suppress the jamming signal without any detailed information of the jamming pattern. With SUAC, it ensures A-SUs' spectrum sensing performance while simultaneously degrades UA-SUs' sensing performance.

B. Communications System Model

In this paper, we consider an OFDM communications architecture in implementing cognitive radio with SUAC. We investigate the OFDM performance under a flat Rayleigh fading channel. Consider a baseband OFDM system with Q subcarriers, among which there are P subcarriers modulated with user data. In the following analysis, denotes p_0 as the first modulated subcarrier index and p_0 to $p_0 + P - 1$ subcarriers are used for data transmissions. Let the k^{th} block corresponding to the $P \times 1$ PU data vector be $\boldsymbol{\theta}(k) = [\theta_0(k), \theta_1(k), \cdots, \theta_{P-1}(k)]^T$, where $\theta_i(k)$ are i.i.d. random variables with zero mean and variance σ_θ^2. Denote a $Q \times Q$ inverse fast Fourier transform (IFFT) matrix $\mathbf{F}_Q$ with the $(i, j)^{\text{th}}$ element as $\frac{1}{\sqrt{Q}} e^{\frac{j2\pi(i-1)(j-1)}{Q}}$. The time domain signal vector after IFFT implementation $[x_0(k), x_1(k), \cdots, x_{Q-1}(k)]^T = \mathbf{F}\boldsymbol{\theta}(k)$, where $\mathbf{F}$ is a $Q \times P$ partial IFFT matrix

$$\mathbf{F} = \mathbf{C}_Q \mathbf{F}_Q \begin{bmatrix} \mathrm{I}_P \\ \mathbf{0}_{(Q-P)\times P} \end{bmatrix}_{Q \times P} \tag{1}$$

where $\mathbf{C}_Q = \text{diag}\left(e^{\frac{j2\pi p_0 i}{Q}}\right)$ is a $Q \times Q$ diagonal matrix, I_P is a $P \times P$ identity matrix and $\mathbf{0}_{(Q-P)\times P}$ is a $(Q-P) \times P$ null matrix.

In order to mitigate inter-block interference (IBI), cyclic prefix (CP) is inserted between successive symbols and the CP length is D. After IFFT operation including inserting CP between successive symbols, the signal can be expressed as

$$\begin{aligned} \mathbf{x}(k) &= [x_{Q-D}(k), \cdots, x_{Q-1}(k), x_0(k), x_1(k), \cdots, x_{Q-1}(k)]^T \\ &= \underbrace{\begin{bmatrix} \left[\mathbf{0}_{D\times(Q-D)}, \mathrm{I}_D\right]\mathbf{F} \\ \mathbf{F} \end{bmatrix}}_{\bar{\mathbf{F}}} \boldsymbol{\theta}(k) = \bar{\mathbf{F}}\boldsymbol{\theta}(k) \end{aligned} \tag{2}$$

Due to the multipath effect, the resulting output signal vector $\mathbf{y}(k)$ can be expressed as

$$\mathbf{y}(k) = \mathbf{H}\bar{\mathbf{F}}\boldsymbol{\theta}(k) + \mathbf{n}(k) \tag{3}$$

where $\mathbf{H}$ is a $(Q + D - L) \times (Q + D)$ Toeplitz matrix constructed from the channel vector $\mathbf{h} = [h_0, h_1, \cdots, h_L]^T$ and can be expressed as

$$\mathbf{H} = \begin{bmatrix} h_0 & \cdots & h_L & & \\ & h_0 & \cdots & h_L & \\ & & \ddots & & \ddots \\ & & & h_0 & \cdots h_L \end{bmatrix} \tag{4}$$

where L denotes the number of multipath components, and $\mathbf{n}(k)$ is a background noise vector with a complex normal distribution $\mathbf{n}(k) \sim \mathcal{CN}\left(0, \sigma_n^2 \mathbf{I}\right)$, where σ_n^2 is noise variance.

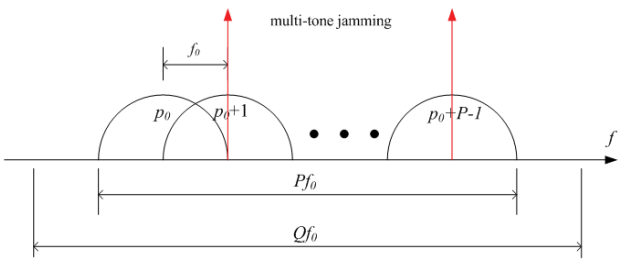

Fig. 2. PU signal and jamming in OFDM.

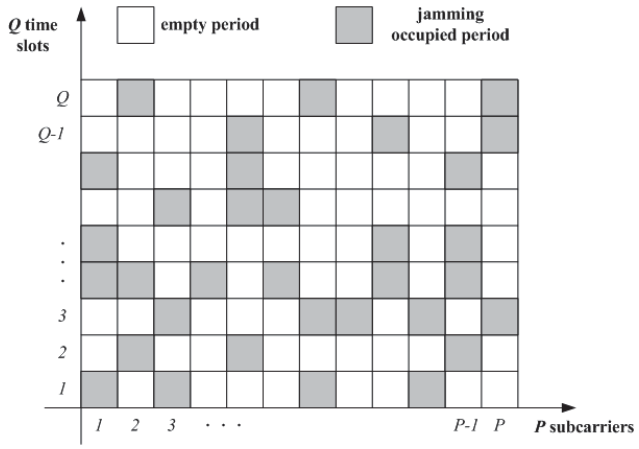

Fig. 3. Illustration of a jamming pattern.

Denote an output signal vector of M blocks as $\mathbf{y}_M = [\mathbf{y}(k-M+1)^T, \mathbf{y}(k-M+2)^T, \cdots, \mathbf{y}(k)^T]^T$ and we have

$$\begin{aligned}\mathbf{y}_M(k) &= \underbrace{\begin{bmatrix} h_0 & \cdots & h_L & & \\ & h_0 & \cdots & h_L & \\ & & \ddots & & \ddots \\ & & & h_0 & \cdots h_L \end{bmatrix}}_{\mathcal{H}_{((Q+D)M-L)\times((Q+D)M)}} \\ &\quad \cdot \underbrace{\begin{bmatrix} \bar{\mathbf{F}} & & & \\ & \bar{\mathbf{F}} & & \\ & & \ddots & \\ & & & \bar{\mathbf{F}} \end{bmatrix}}_{\mathcal{F}} \underbrace{\begin{bmatrix} \boldsymbol{\theta}(k-M+1) \\ \boldsymbol{\theta}(k-M+2) \\ \vdots \\ \boldsymbol{\theta}(k) \end{bmatrix}}_{\widetilde{\boldsymbol{\theta}}(k)} \\ &\quad + \underbrace{\begin{bmatrix} \mathbf{n}(k-M+1) \\ \mathbf{n}(k-M+2) \\ \vdots \\ \mathbf{n}(k) \end{bmatrix}}_{\widetilde{\mathbf{n}}(k)} \\ &= \mathcal{H}\mathcal{F}\widetilde{\boldsymbol{\theta}}(k) + \widetilde{\mathbf{n}}(k) \end{aligned} \tag{5}$$

In the frequency domain, the spectrum of a PU signal and a multi-tone jammer are illustrated in Fig. 2 and Fig. 3. The entire band is divided into Q orthogonal subchannels and P sub-channels modulated with the user data. The space between adjacent subchannels is $f_0 = \frac{1}{T}$, where T is the symbol interval. The total bandwidth of Q sub-channels is Qf_0. For the multi-tone jammer, it generates a jamming signal with total power P_J at multiple subchannels within P modulated sub-channels (Fig. 2). During each symbol interval, the jammer may hop or choose different subchannels to transmit (Fig. 3). When considering the effect of multi-tone jamming, (3) can be rewritten as

$$\mathbf{y}(k) = \underbrace{\mathbf{H}\bar{\mathbf{F}}\boldsymbol{\theta}(k)}_{\text{signal part}} + \underbrace{\mathbf{H}\bar{\mathbf{F}}_J\boldsymbol{\phi}(k)}_{\text{jamming part}} + \mathbf{n}(k) \tag{6}$$

where $\boldsymbol{\phi}(k) = [\phi_0(k), \phi_1(k), \cdots, \phi_{P-1}(k)]^T$ represents the k^{th} block jamming data vector and $\phi_i(k)$ are i.i.d. random variables with zero mean and variance σ_ϕ^2. The jamming matrix $\bar{\mathbf{F}}_J$ can be expressed as

$$\bar{\mathbf{F}}_J = \begin{bmatrix} \left[\mathbf{0}_{D\times(Q-D)}, \mathrm{I}_D\right] \cdot (\mathbf{F} * \Delta) \\ \mathbf{F} * \Delta \end{bmatrix}_{(Q+D)\times P} \tag{7}$$

where Δ is a $Q \times P$ dimension full rank jamming pattern matrix and the $(i, j)^{\text{th}}$ element δ_{ij} equals to 1 or 0. $\delta_{ij} = 1$ denotes that the jammer occupies j^{th} subchannel in i^{th} symbol interval, otherwise, $\delta_{ij} = 0$. This jamming pattern (δ_{ij} values) is available only to the A-SUs. $\mathbf{F} * \Delta$ is the Hadamard product of $\mathbf{F}$ and Δ. Then the output signal vector of M blocks can be expressed as

$$\begin{aligned}\mathbf{y}_M(k) &= \mathcal{H}\mathcal{F}\widetilde{\boldsymbol{\theta}}(k) + \mathcal{H}\underbrace{\left(\bar{\mathbf{F}}_J \otimes \mathbf{I}_M\right)}_{\mathcal{F}_J} \underbrace{\begin{bmatrix} \boldsymbol{\phi}(k-M+1) \\ \boldsymbol{\phi}(k-M+2) \\ \vdots \\ \boldsymbol{\phi}(k) \end{bmatrix}}_{\widetilde{\boldsymbol{\phi}}(k)} + \widetilde{\mathbf{n}}(k) \\ &= \underbrace{\mathcal{H}\mathcal{F}}_{\mathcal{A}}\widetilde{\boldsymbol{\theta}}(k) + \underbrace{\mathcal{H}\mathcal{F}_J}_{\mathcal{B}}\widetilde{\boldsymbol{\phi}}(k) + \widetilde{\mathbf{n}}(k) \end{aligned} \tag{8}$$

Matrices $\mathcal{A}$ and $\mathcal{B} \in \mathbb{C}^{((Q+D)M-L)\times PM}$ and both have full rank. In our SUAC design, it is required that the composite matrix $[\mathcal{A}\,\mathcal{B}] \in \mathbb{C}^{((Q+D)M-L)\times 2PM}$ has full column rank which implies that $\mathcal{A}$ and $\mathcal{B}$ are disjoint or non-overlapping. In order to meet this condition, a necessary condition is that $(Q + D - 2P)\,M - L \geq 0$ (Condition I) is required. Assume Condition I is satisfied, the rank of $[\mathcal{A}\,\mathcal{B}]$ is $\min\{2PM,\ QM\}$. Since matrix $[\mathcal{A}\,\mathcal{B}]$ has full column rank $(2PM)$, we have $2PM \leq QM$, which implies that $2P \leq Q$ (Condition II). Both Condition I and II are required in our SUAC design. Notice that disjoint does not imply orthogonal and orthogonality is a much stronger condition. In our design, we do not require that $\mathcal{A}$ is orthogonal to $\mathcal{B}$. Notice that there is added complexity due to the jamming generation. The computational complexity is determined/limited by jamming pattern matrix size, which is related to the number of OFDM subcarriers.

III. Oblique Projection and GLRT Based PU Detection Approach

In this section, we analyze a channel estimation approach for both authorized and unauthorized SUs and a GLRT based PU detection approach is introduced. In the following, we will first review the oblique projection technique in matrix theory [25], which will be used in the GLRT based detection.

A. Oblique Projection

We review the equations related to a projection matrix. The well known formula to construct an orthogonal projection with range span $(\mathcal{A})$ is $\mathbf{P}_{\mathcal{A}} = \mathcal{A}\left(\mathcal{A}^H\mathcal{A}\right)^{-1}\mathcal{A}^H$ and the orthogonal projection with range Null $(\mathcal{A})$ is $\mathbf{P}_{\mathcal{A}}^{\perp} = \mathbf{I} - \mathbf{P}_{\mathcal{A}}$. Typically the orthogonal projection of $\mathbf{y}$ onto span $([\mathcal{A}\,\mathcal{B}])$ is denoted as $\mathbf{P}_{\mathcal{A}\mathcal{B}}\mathbf{y}$ and $\mathbf{P}_{\mathcal{A}\mathcal{B}}$ can be written as

$$\mathbf{P}_{\mathcal{A}\mathcal{B}} = [\mathcal{A}\,\mathcal{B}][[\mathcal{A}\,\mathcal{B}]^H[\mathcal{A}\,\mathcal{B}]]^{-1}[\mathcal{A}\,\mathcal{B}]^H \tag{9}$$

which can be decomposed with respect to signal subspace span $(\mathcal{A})$ and jamming subspace span $(\mathcal{B})$ as

$$\mathbf{P}_{\mathcal{A}\mathcal{B}} = \mathbf{E}_{\mathcal{A}\mathcal{B}} + \mathbf{E}_{\mathcal{B}\mathcal{A}} \tag{10}$$

where the orthogonal projection $\mathbf{P}_{\mathcal{A}\mathcal{B}}$ is decomposed into oblique projections $\mathbf{E}_{\mathcal{A}\mathcal{B}}$ and $\mathbf{E}_{\mathcal{B}\mathcal{A}}$, with $\mathbf{E}_{\mathcal{A}\mathcal{B}} = \mathcal{A}\left(\mathcal{A}^H\mathbf{P}_{\mathcal{B}}^{\perp}\mathcal{A}\right)^{-1}\mathcal{A}^H\mathbf{P}_{\mathcal{B}}^{\perp}$ and $\mathbf{E}_{\mathcal{B}\mathcal{A}} = \mathcal{B}\left(\mathcal{B}^H\mathbf{P}_{\mathcal{A}}^{\perp}\mathcal{B}\right)^{-1}\mathcal{B}^H\mathbf{P}_{\mathcal{A}}^{\perp}$, respectively [25].

B. Channel Estimation for SU (A-SU and UA-SU)

In the SUAC communications model, by using the subspace-based blind channel estimation algorithm [26], both authorized and unauthorized SUs can achieve desired channel estimation results. Notice that this is different from a physical layer security transmission model, which relies on utilizing communication channel characteristics to guarantee secure transmissions.

From (8) we know that both matrix $\mathcal{A}$ and $\mathcal{B}$ contain the channel matrix $\mathcal{H}$. After collecting N_e output signal vector $\mathbf{y}_M(k)$, we have

$$\begin{aligned}\mathbf{Y} &= [\mathbf{y}_M(1), \mathbf{y}_M(2), \cdots, \mathbf{y}_M(N_e)] \\ &= [\mathcal{A}\,\mathcal{B}]\begin{bmatrix}\widetilde{\boldsymbol{\theta}}(1) & \widetilde{\boldsymbol{\theta}}(2) & \cdots & \widetilde{\boldsymbol{\theta}}(N_e) \\ \widetilde{\boldsymbol{\phi}}(1) & \widetilde{\boldsymbol{\phi}}(2) & \cdots & \widetilde{\boldsymbol{\phi}}(N_e)\end{bmatrix} \\ &\quad + [\widetilde{\mathbf{n}}(1), \widetilde{\mathbf{n}}(2), \cdots, \widetilde{\mathbf{n}}(N_e)]\end{aligned} \tag{11}$$

Take the singular value decomposition (SVD) on the received signal matrix $\mathbf{Y}$ and we have

$$\mathbf{Y} = [\mathbf{U}_s\ \mathbf{U}_n]\begin{bmatrix}\boldsymbol{\Sigma}_s & \\ & \boldsymbol{\Sigma}_n\end{bmatrix}\begin{bmatrix}\mathbf{U}_s^H \\ \mathbf{U}_n^H\end{bmatrix} \tag{12}$$

where matrix $\mathbf{U}_s \in \mathbb{C}^{((Q+D)M-L)\times PM}$ spans the signal subspace and matrix $\mathbf{U}_n$ with the dimension $\mathbb{C}^{((Q+D)M-L)\times((Q+D-P)M-L)}$ spans the noise subspace. $\boldsymbol{\Sigma}_s$ and $\boldsymbol{\Sigma}_n$ are diagonal matrices consisting singular values corresponding to $\mathbf{U}_s$ and $\mathbf{U}_n$. Denote $\mathbf{U}_n(i)$ as the i^{th} column of $\mathbf{U}_n$ and, from the orthogonality between signal and noise subspace, we have

$$\mathbf{U}_n(i)^H \cdot [\mathcal{A}\,\mathcal{B}] \approx 0 \tag{13}$$

Channel vector $\mathbf{h}$ can be estimated by using (12) [26],

$$\hat{\mathbf{h}} = \arg\min_{\|\hat{\mathbf{h}}\|=1}\left(\hat{\mathbf{h}}^*\right)^H\hat{\mathcal{G}}\hat{\mathcal{G}}^H\left(\hat{\mathbf{h}}^*\right) \tag{14}$$

$\hat{\mathcal{G}}$ is the estimate of $\mathcal{G}$ and $\mathcal{G} = [\mathbf{G}_1, \cdots, \mathbf{G}_{(Q+D-P)M-L}]$. $\mathbf{G}_i$ is given as

$$\mathbf{G}_i = \begin{bmatrix}\mathbf{U}_n(i)^T & & & \\ & \mathbf{U}_n(i)^T & & \\ & & \ddots & \\ & & & \mathbf{U}_n(i)^T\end{bmatrix}_{(L+1)\times(Q+D)M} \cdot[\mathcal{F}\ \mathcal{F}_J] \tag{15}$$

By carrying out SVD of matrix $\hat{\mathcal{G}}\hat{\mathcal{G}}^H$, we have $\hat{\mathcal{G}}\hat{\mathcal{G}}^H = \mathbf{U}_{\mathcal{G}}\mathbf{V}_{\mathcal{G}}\mathbf{U}_{\mathcal{G}}^H$ and the diagonal matrix $\mathbf{V}_{\mathcal{G}} = \text{diag}[\lambda_1, \cdots, \lambda_L + 1]$ are in a descending order. The solution of this optimization problem is achieved when $\hat{\mathbf{h}}^* = \mathbf{U}_{\mathcal{G}}[:, L+1]$.

C. GLRT Based PU Detection Approach for A-SU

Considering a complex Gaussian model [4], the PU detection problem (spectrum sensing) for an A-SU is as follows,

$$\mathbb{H}_0 : \mathbf{y}_M \sim \mathcal{CN}[\mathcal{B}\widetilde{\boldsymbol{\phi}}, \sigma_n^2\mathbf{I}] \tag{16}$$

$$\mathbb{H}_1 : \mathbf{y}_M \sim \mathcal{CN}[\mathcal{A}\widetilde{\boldsymbol{\theta}} + \mathcal{B}\widetilde{\boldsymbol{\phi}}, \sigma_n^2\mathbf{I}] \tag{17}$$

As indicated in (8), $\mathcal{A}$ is composed of a well known IFFT matrix $\mathbf{F}_Q$ and channel matrix $\mathcal{H}$, while $\mathcal{B}$ contains Δ which is only known by the A-SUs. GLRT decides $\mathbb{H}_1$ if the likelihood ratio $L(\mathbf{y}_M)$ exceeds a threshold γ:

$$L(\mathbf{y}_M) = \frac{p\left(\mathbf{y}_M; \ddot{\boldsymbol{\theta}}, \ddot{\boldsymbol{\phi}}, \mathbb{H}_1\right)}{p\left(\mathbf{y}_M; \ddot{\boldsymbol{\phi}}, \mathbb{H}_0\right)} > \gamma \tag{18}$$

Since $\ddot{\boldsymbol{\theta}}$ $(\ddot{\boldsymbol{\phi}})$ is the maximum likelihood estimation (MLE) of $\widetilde{\boldsymbol{\theta}}$ $(\widetilde{\boldsymbol{\phi}})$ under $\mathbb{H}_1/\mathbb{H}_0$, (18) can be written as

$$L(\mathbf{y}_M) = \frac{\max\limits_{\widetilde{\boldsymbol{\theta}}, \widetilde{\boldsymbol{\phi}}} p\left(\mathbf{y}_M; \widetilde{\boldsymbol{\theta}}, \widetilde{\boldsymbol{\phi}}, \mathbb{H}_1\right)}{\max\limits_{\widetilde{\boldsymbol{\phi}}} p\left(\mathbf{y}_M; \widetilde{\boldsymbol{\phi}}, \mathbb{H}_0\right)} > \gamma \tag{19}$$

From [22], we have

$$\begin{aligned}\ln L(\mathbf{y}_M) &= \frac{1}{\sigma_n^2}\mathbf{y}_M^H\left(\mathbf{P}_{\mathcal{B}}^{\perp} - \mathbf{P}_{\mathcal{A}\mathcal{B}}^{\perp}\right)\mathbf{y}_M \\ &= \frac{1}{\sigma_n^2}\mathbf{y}_M^H\mathbf{P}_{\mathbf{P}_{\mathcal{B}}^{\perp}\mathcal{A}}\mathbf{y}_M > \ln\gamma\end{aligned} \tag{20}$$

The detector can be further written as

$$T(\mathbf{y}_M) = \mathbf{y}_M^H\mathbf{P}_{\mathbf{P}_{\mathcal{B}}^{\perp}\mathcal{A}}\mathbf{y}_M > \gamma' \tag{21}$$

which is χ^2 distributed,

$$\mathbb{H}_0 : T(\mathbf{y}_M) \sim \sigma_n^2\chi_{2PM}^2(0) \tag{22}$$

$$\mathbb{H}_1 : T(\mathbf{y}_M) \sim \sigma_n^2\chi_{2PM}^2\left(\widetilde{\boldsymbol{\theta}}^H\mathcal{A}^H\mathbf{P}_{\mathbf{P}_{\mathcal{B}}^{\perp}\mathcal{A}}\mathcal{A}\widetilde{\boldsymbol{\theta}}\right) \tag{23}$$

D. GLRT Based PU Detection Approach for UA-SU

Without knowing the jamming pattern matrix $\boldsymbol{\Delta}$, a UA-SU is unable to obtain the corresponding orthogonal/oblique projection operators ($\mathbf{P}_{\mathcal{B}}^{\perp}$ and $\mathbf{P}_{\mathbf{P}_{\mathcal{B}}^{\perp}\mathcal{A}}$). However, following [23], a UA-SU is able to use an alternative approach to detect a PU signal.

Assuming that PU signal vector $\widetilde{\boldsymbol{\theta}}$, jamming signal vector $\widetilde{\boldsymbol{\phi}}$ and noise vector $\widetilde{\mathbf{n}}$ are mutually independent, the output signal covariance matrix $\mathbf{R}_{\mathbf{y}_M\mathbf{y}_M}$ can be written as

$$\begin{aligned}\mathbf{R}_{\mathbf{y}_M\mathbf{y}_M} &= \mathcal{A}\mathbf{R}_{\widetilde{\boldsymbol{\theta}}\widetilde{\boldsymbol{\theta}}}\mathcal{A}^H + \mathcal{B}\mathbf{R}_{\widetilde{\boldsymbol{\phi}}\widetilde{\boldsymbol{\phi}}}\mathcal{B}^H + \sigma_n^2\mathbf{I} \\ &= [\mathcal{A}\,\mathcal{B}]\begin{bmatrix}\mathbf{R}_{\widetilde{\boldsymbol{\theta}}\widetilde{\boldsymbol{\theta}}} & \mathbf{0} \\ \mathbf{0} & \mathbf{R}_{\widetilde{\boldsymbol{\phi}}\widetilde{\boldsymbol{\phi}}}\end{bmatrix}\begin{bmatrix}\mathcal{A}^H \\ \mathcal{B}^H\end{bmatrix} + \sigma^2\mathbf{I} \\ &= \mathbf{S}\mathbf{Q}\mathbf{S}^H + \sigma_n^2\mathbf{I} \\ &= \mathbf{R}_{\mathbf{S}} + \sigma_n^2\mathbf{I} \end{aligned} \tag{24}$$

where $\mathbf{S} = [\mathcal{A}\,\mathcal{B}]$, $\mathbf{Q} = \text{diag}\{\mathbf{R}_{\widetilde{\boldsymbol{\theta}}\widetilde{\boldsymbol{\theta}}}, \mathbf{R}_{\widetilde{\boldsymbol{\phi}}\widetilde{\boldsymbol{\phi}}}\}$ and $\mathbf{R}_{\mathbf{S}} = \mathbf{S}\mathbf{Q}\mathbf{S}^H$.

The pseudo-inverse of matrix $\mathbf{S}$ is [25]

$$\mathbf{S}^\dagger = [\mathcal{A}\,\mathcal{B}]^\dagger = \begin{bmatrix}\left(\mathcal{A}^H\mathbf{P}_{\mathcal{B}}^\perp\mathcal{A}\right)^{-1}\mathcal{A}^H\mathbf{P}_{\mathcal{B}}^\perp \\ \left(\mathcal{B}^H\mathbf{P}_{\mathcal{A}}^\perp\mathcal{B}\right)^{-1}\mathcal{B}^H\mathbf{P}_{\mathcal{A}}^\perp\end{bmatrix} \tag{25}$$

and the pseudo-inverse matrix of $\mathbf{R}_{\mathbf{S}}$ is

$$\mathbf{R}_{\mathbf{S}}^\dagger = \left(\mathbf{S}^\dagger\right)^H\mathbf{Q}^{-1}\mathbf{S}^\dagger \tag{26}$$

From (26), we have

$$\begin{aligned}\mathbf{R}_{\mathbf{S}}^\dagger\mathcal{A} &= \left(\mathbf{S}^\dagger\right)^H\mathbf{Q}^{-1}\mathbf{S}^\dagger\mathcal{A} \\ &= \left(\mathbf{S}^\dagger\right)^H\mathbf{Q}^{-1}\begin{bmatrix}\left(\mathcal{A}^H\mathbf{P}_{\mathcal{B}}^\perp\mathcal{A}\right)^{-1}\mathcal{A}^H\mathbf{P}_{\mathcal{B}}^\perp \\ \left(\mathcal{B}^H\mathbf{P}_{\mathcal{A}}^\perp\mathcal{B}\right)^{-1}\mathcal{B}^H\mathbf{P}_{\mathcal{A}}^\perp\end{bmatrix}\mathcal{A} \\ &= \mathbf{P}_{\mathcal{B}}^\perp\mathcal{A}\left(\mathcal{A}^H\mathbf{P}_{\mathcal{B}}^\perp\mathcal{A}\right)^{-1}\mathbf{R}_{\widetilde{\boldsymbol{\theta}}\widetilde{\boldsymbol{\theta}}}^{-1}\end{aligned} \tag{27}$$

Further,

$$\begin{aligned}\mathbf{P}_{\mathbf{R}_{\mathbf{S}}^\dagger\mathcal{A}} &= \mathbf{R}_{\mathbf{S}}^\dagger\mathcal{A}\left(\mathcal{A}^H\mathbf{R}_{\mathbf{S}}^\dagger\mathbf{R}_{\mathbf{S}}^\dagger\mathcal{A}\right)^{-1}\mathcal{A}^H\mathbf{R}_{\mathbf{S}}^\dagger \\ &= \mathbf{P}_{\mathcal{B}}^\perp\mathcal{A}\left(\mathcal{A}^H\mathbf{P}_{\mathcal{B}}^\perp\mathcal{A}\right)^{-1}\mathcal{A}^H\mathbf{P}_{\mathcal{B}}^\perp \\ &= \mathbf{P}_{\mathbf{P}_{\mathcal{B}}^\perp\mathcal{A}}\end{aligned} \tag{28}$$

This concludes that $\mathbf{P}_{\mathbf{R}_{\mathbf{S}}^\dagger\mathcal{A}} = \mathbf{P}_{\mathbf{P}_{\mathcal{B}}^\perp\mathcal{A}}$ if signal vector $\widetilde{\boldsymbol{\theta}}$ is independent of jamming vector $\widetilde{\boldsymbol{\phi}}$. Therefore, a detector for the UA-SU can be written as

$$T(\mathbf{y}_M) = \mathbf{y}_M^H\mathbf{P}_{\mathbf{R}_{\mathbf{S}}^\dagger\mathcal{A}}\mathbf{y}_M \tag{29}$$

and $T(\mathbf{y}_M)$ is χ^2 distributed,

$$\mathbb{H}_0 : T(\mathbf{y}_M) \sim \sigma_n^2\chi_{2PM}^2(0) \tag{30}$$

$$\mathbb{H}_1 : T(\mathbf{y}_M) \sim \sigma_n^2\chi_{2PM}^2\left(\widetilde{\boldsymbol{\theta}}^H\mathcal{A}^H\mathbf{P}_{\mathbf{R}_{\mathbf{S}}^\dagger\mathbf{H}}\mathcal{A}\widetilde{\boldsymbol{\theta}}\right) \tag{31}$$

E. Performance Comparison Between Authorized and Unauthorized SU

We use the deflection coefficient d^2 [21], to evaluate the detection performance of an A-SU and a UA-SU, which is defined as

$$d^2 = \frac{\left(\text{E}(T \mid \mathbb{H}_1) - \text{E}(T \mid \mathbb{H}_0)\right)^2}{\text{Var}(T \mid \mathbb{H}_0)} \tag{32}$$

For the A-SU, from (22) and (23), we have

$$\text{E}(T \mid \mathbb{H}_1) = 2PM + \widetilde{\boldsymbol{\theta}}^H\mathcal{A}^H\mathbf{P}_{\mathbf{P}_{\mathcal{B}}^\perp\mathcal{A}}\mathcal{A}\widetilde{\boldsymbol{\theta}} \tag{33}$$

$$\text{E}(T \mid \mathbb{H}_0) = 2PM \tag{34}$$

$$\text{Var}(T \mid \mathbb{H}_0) = 4PM \tag{35}$$

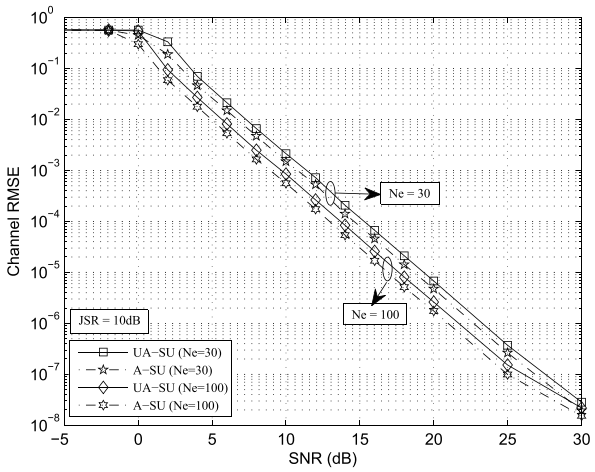

Fig. 4. A-SU and UA-SU's channel RMSE versus SNR for different N_e, given JSR = 10 dB.

and the deflection coefficient for the A-SU is

$$d_1^2 = \frac{\left(\widetilde{\boldsymbol{\theta}}^H\mathcal{A}^H\mathbf{P}_{\mathbf{P}_{\mathcal{B}}^\perp\mathcal{A}}\mathcal{A}\widetilde{\boldsymbol{\theta}}\right)^2}{4P} \tag{36}$$

Similarly, the deflection coefficient for the UA-SU can be found as

$$d_2^2 = \frac{\left(\widetilde{\boldsymbol{\theta}}^H\mathcal{A}^H\mathbf{P}_{\mathbf{R}_{\mathbf{S}}^\dagger\mathcal{A}}\mathcal{A}\widetilde{\boldsymbol{\theta}}\right)^2}{4P} \tag{37}$$

and it is seen that the detection performance for authorized and unauthorized SU will highly depend on $\mathbf{P}_{\mathbf{P}_{\mathcal{B}}^\perp\mathcal{A}}$ and $\mathbf{P}_{\mathbf{R}_{\mathbf{S}}^\dagger\mathcal{A}}$. It can be shown that d_1^2 is much larger than d_2^2 if a UA-SU is unable to obtain an accurate estimation of $\mathbf{P}_{\mathbf{P}_{\mathcal{B}}^\perp\mathcal{A}}$.

IV. Simulation Results and Related Discussions

In this section, the simulation results of the proposed SUAC method are presented. We consider an OFDM system with binary phase shift keying (BPSK) modulation, given the number of subcarriers $Q = 15$, the number of modulated subcarriers $P = 7$, CP length $D = 4$, the number of multipath components $L = 3$ and the number of blocks $M = 2$. Notice that both Condition I ($(Q + D - 2P)M \geq L$) and Condition II ($2P \leq Q$) are satisfied. Signal vector $\widetilde{\boldsymbol{\theta}}$ and jamming vector $\widetilde{\boldsymbol{\phi}}$ are mutually independent. Signal to noise ratio (SNR) and jamming to signal ratio (JSR) are defined as

$$\text{SNR} = 10\log_{10}\left(\frac{P\sigma_\theta^2}{(Q+D)\,\sigma_n^2}\right) \tag{38}$$

$$\text{JSR} = 10\log_{10}\left(\frac{\sigma_\phi^2}{\sigma_\theta^2}\right) \tag{39}$$

Fig. 4 presents A-SU and UA-SU's channel estimation performance versus SNR for different N_e values ($N_e = 30, 100$). Normalized root mean square error (RMSE) is used to evaluate channel estimation performance [26],

$$\text{RMSE} = \sqrt{\frac{1}{N_r(L+1)}\sum_{i=1}^{N_r}\frac{\|\hat{\mathbf{h}}_i - \mathbf{h}_i\|^2}{\|\mathbf{h}_i\|^2}} \tag{40}$$

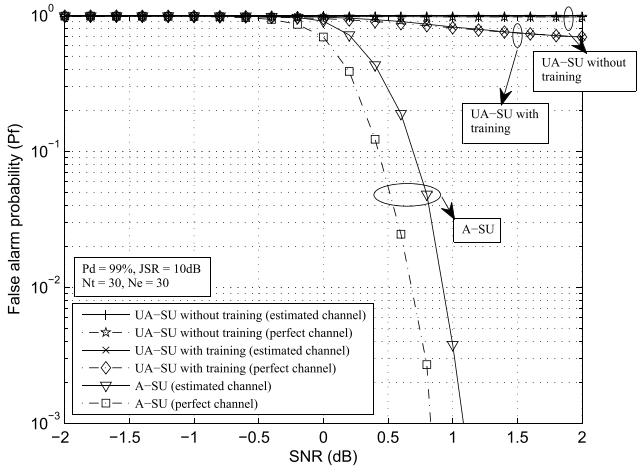

Fig. 5. P_f versus SNR given $P_d = 99\%$, JSR $= 10$ dB, $N_t = 30$ and $N_e = 30$.

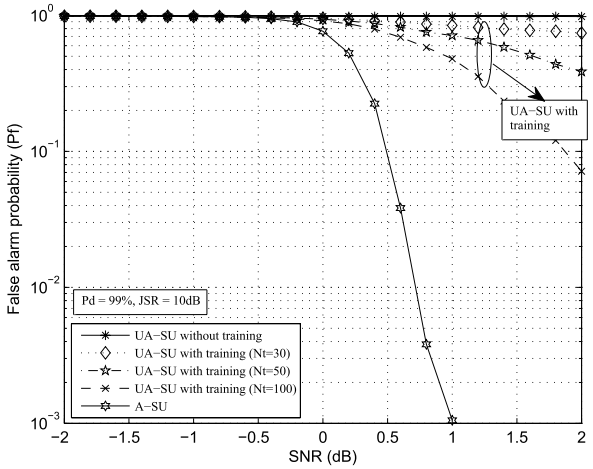

Fig. 6. P_f versus SNR for different N_t, given $P_d = 99\%$, JSR $= 10$ dB and perfect channel state information.

where N_r denotes the number of simulation iterations and i refers to i^{th} simulation results. In our analysis, simulation results are obtained with $N_r = 200$ runs and JSR $=$ 10dB. From Fig. 4, the following observations are made.

1) For both A-SU and UA-SU, the channel estimation performance improves with increasing SNR.

2) Larger N_e leads to better channel estimation performance.

3) In general, A-SU's channel estimation performance outperforms UA-SU. Notice that the performance gap between A-SU and UA-SU is insignificant since for A-SU, from (13), we have $\mathbf{U}_n(i)^H \cdot [\mathcal{A}\,\mathcal{B}] \approx 0$ and $\mathcal{B}$ includes jamming pattern matrix Δ (7). Δ is a $Q \times P$ full rank matrix with elements zero or one. For UA-SUs, without knowing jamming pattern matrix Δ, they can generate arbitrary $Q \times P$ full rank matrix Δ_g with "0" and "1" as its elements, and $\mathbf{U}_n(i)^H \cdot [\mathcal{A}\,\mathcal{B}_g] \approx 0$ can be obtained with $\mathcal{B}_g$ including guessed jamming pattern matrix Δ_g. This indicates that UA-SU can achieve good channel estimation performance without knowing jamming pattern matrix Δ.

In the following figures, we will present SUAC performance results. Notice that, in cognitive radio networks, two important performance measures are primary user detection probability (P_d) and false alarm probability (P_f). Typically, system designs should ensure that P_d is very high (e.g., $P_d \geq 90\%$ under -21 dB for PU SNR [27]) to avoid significant interference to PUs. Also, P_f should be very low so that SUs are able to find and utilize vacant spectrum more efficiently. In our SUAC designs, both A-SU and UA-SU should meet a requirement of high P_d to avoid interference to PUs. However, for P_f, we have different requirements for A-SU and UA-SU. For A-SU, P_f should be very low so that A-SU is able to find and utilize vacant spectrum efficiently. For UA-SU, on the other hand, P_f should be high to prevent UA-SU use of the vacant spectrum, which is the objective of SUAC. Therefore, in the following figures, we compare P_f performance of A-SU versus UA-SU given that P_d is relatively high (e.g., 90%, 99%).

Fig. 5 presents the false alarm probability versus SNR given $P_d = 99\%$, JSR $= 10$ dB and $N_e = 30$. In the simulation results, three different types of SUs are considered: A-SU, UA-SU without training and UA-SU with training.

For an A-SU, the detector presented in (21) is implemented. For a UA-SU without training, SU uses the same detector presented in (21) without knowing accurate $\mathcal{B}$. For a UA-SU with training, the detector shown in (29) is implemented and $\mathbf{R}_{\mathbf{y}_M\mathbf{y}_M}$ is calculated as follows,

$$\mathbf{R}_{\mathbf{y}_M\mathbf{y}_M} \approx \frac{1}{N_t}\mathbf{Y}_{N_t}\mathbf{Y}_{N_t}^H \tag{41}$$

where $\mathbf{Y}_{N_t} = [\mathbf{y}_M(1), \mathbf{y}_M(2), \cdots, \mathbf{y}_M(N_t)]$. In Fig. 4, simulation results are given with $N_t = 30$. Both perfect channel estimation and estimated channel with $N_e = 30$ are considered for authorized and unauthorized SUs (with or without training). From the simulation results, we have the following observations.

1) For both authorized and unauthorized SUs, P_f performance improves with an increasing SNR value.

2) In order to achieve the same P_f performance, higher SNR is needed when using estimated channel information.

3) There is a significant performance gap between authorized and unauthorized SUs. For instance, when SNR $= 1$ dB and considering estimated channel information, P_f of an A-SU equals to 0.7% while P_f of a UA-SU with training equals to approximately 80% and a UA-SU without training equals to more than 90%. This demonstrates that SUAC is an effective method in spectrum access control.

Fig. 6 presents the false alarm probability versus SNR, given $P_d = 99\%$, JSR $= 10$ dB and perfect channel state information, for various UA-SU detection training size N_t. From the figure, we have the following observations. 1) The detection performance varies from the worst to the best in the following order: UA-SU without training, UA-SU with training and A-SU.

2) Considering UA-SU with training, the detection performance improves with increasing N_t.

Fig. 7 presents the false alarm probability versus SNR, given $N_t = 30$, JSR $= 10$ dB and perfect channel state information,

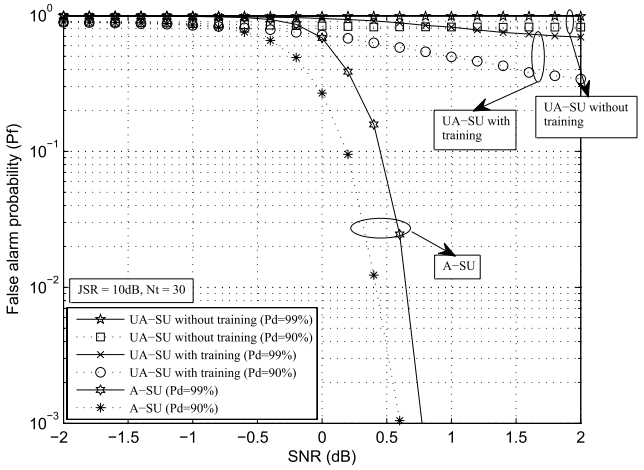

Fig. 7. P_f versus SNR for different P_d, given $N_t = 30$, JSR $= 10$ dB and perfect channel state information.

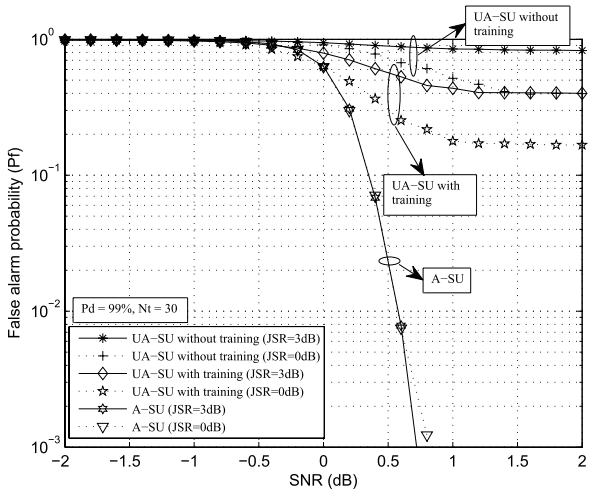

Fig. 8. P_f versus SNR for different JSR, given $P_d = 99\%$, $N_t = 30$ and perfect channel state information.

for various detection probability P_d. From the figure, we have the following observations.

1) The detection performance varies from the worst to the best in the following order: UA-SU without training, UA-SU with training and A-SU.

2) In order to achieve the same P_f performance, larger SNR is needed when P_d is higher.

Fig. 8 presents the false alarm probability versus SNR, given $N_t = 30$, $P_d = 99\%$ and perfect channel state information, for various JSR. From the figure, we have the following observations.

1) The detection performance varies from the worst to the best in the following order: UA-SU without training, UA-SU with training and A-SU.

2) Considering UA-SU with and without training, the detection performance degrades with increasing JSR, which achieves the objective of SUAC. However, extra power consumption incurs due to jamming.

3) For A-SU, the detection performance does not depend on JSR values due to jamming cancellation.

V. Conclusions

In this paper, we have investigated an SUAC technique considering an OFDM communication architecture. For both authorized and unauthorized SUs, the GLRT based algorithm is used for PU detection (spectrum sensing). With the knowledge/information of the jamming sequence features and applying the oblique projection technique, A-SUs are able to achieve reliable sensing performance. However, the sensing performance of UA-SUs are significantly degraded due to the jamming signal.

References

[1] J. Mitola and G. Q. Maguire, "Cognitive radio: Making software radios more personal," *IEEE Pers. Commun.*, vol. 6, no. 4, pp. 13–18, Apr. 1999.

[2] J. Unnikrishnan and V. V. Veeravalli, "Cooperative sensing for primary detection in cognitive radio," *IEEE J. Sel. Topics Signal Process.*, vol. 2, no. 1, pp. 18–27, Feb. 2008.

[3] G. Ding, Q. Wu, Y.-D. Yao, J. Wang, and Y. Chen, "Kernel-based learning for statistical signal processing in cognitive radio networks: Theoretical foundations, example applications, and future directions," *IEEE Signal Process. Mag.*, vol. 30, no. 4, pp. 126–136, Jul. 2013.

[4] P. Wang, J. Fang, N. Han, and H. Li, "Multiantenna-assisted spectrum sensing for cognitive radio," *IEEE Trans. Veh. Technol.*, vol. 59, no. 4, pp. 1791–1800, May 2010.

[5] Y. Zeng and Y.-C. Liang, "Eigenvalue-based spectrum sensing algorithms for cognitive radio," *IEEE Trans. Commun.*, vol. 57, no. 6, pp. 1784–1793, Jun. 2009.

[6] H. Lee, S. Vahid, and K. Moessner, "A survey of radio resource management for spectrum aggregation in LTE-advanced," *IEEE Commun. Surveys Tuts.*, vol. 16, no. 2, pp. 745–760, 2nd Quart., 2014.

[7] G. Ding, J. Wang, Q. Wu, Y.-D. Yao, F. Song, and T. Tsiftsis, "Cellular-base-station-assisted device-to-device communications in TV white space," *IEEE J. Sel. Areas Commun.*, vol. 34, no. 1, pp. 107–121, Jan. 2016.

[8] R. Chen, J. M. Park, and J. H. Reed, "Defense against primary user emulation attacks in cognitive radio networks," *IEEE J. Sel. Areas Commun.*, vol. 26, no. 1, pp. 25–37, Jan. 2008.

[9] N. Hu, Y.-D. Yao, and J. Mitola, "Most active band (MAB) attack and countermeasures in a cognitive radio network," *IEEE Trans. Wireless Commun.*, vol. 11, no. 3, pp. 898–902, Mar. 2012.

[10] R. Chen, J. M. Park, Y. T. Hou, and J. H. Reed, "Toward secure distributed spectrum sensing in cognitive radio networks," *IEEE Commun. Mag.*, vol. 46, no. 4, pp. 50–55, Apr. 2008.

[11] D. Niyato and E. Hossain, "Competitive pricing for spectrum sharing in cognitive radio networks: Dynamic game, inefficiency of Nash equilibrium, and collusion," *IEEE J. Sel. Areas Commun.*, vol. 26, no. 1, pp. 192–202, Jan. 2008.

[12] D. Niyato, E. Hossain, and Z. Han, "Dynamics of multiple-seller and multiple-buyer spectrum trading in cognitive radio networks: A game-theoretic modeling approach," *IEEE Trans. Mobile Comput.*, vol. 8, no. 8, pp. 1009–1022, Aug. 2009.

[13] H. Wang, Y.-D. Yao, R. Wang, and L. Shen, "Coordinated jamming and communications in an MC-CDMA system," *IEEE Trans. Aerosp. Electron. Syst.*, vol. 51, no. 4, pp. 3151–3160, Oct. 2015.

[14] A. Mukherjee, S. Fakoorian, J. Huang, and A. Swindlehurst, "Principles of physical layer security in multiuser wireless networks: A survey," *IEEE Commun. Surveys Tuts.*, vol. 16, no. 3, pp. 1550–1573, 3rd Quart., 2014.

[15] S. Goel and R. Negi, "Guaranteeing secrecy using artificial noise," *IEEE Trans. Wireless Commun.*, vol. 7, no. 6, pp. 2180–2189, Jun. 2008.

[16] L. Dong, Z. Han, A. Petropulu, and H. V. Poor, "Improving wireless physical layer security via cooperating relays," *IEEE Trans. Signal Process.*, vol. 58, no. 3, pp. 1875–1888, Mar. 2010.

[17] L. Zhang, R. Zhang, Y.-C. Liang, Y. Xin, and S. Cui, "On the relationship between the multi-antenna secrecy communications and cognitive radio communications," *IEEE Trans. Commun.*, vol. 58, no. 6, pp. 1877–1886, Jun. 2010.

[18] V. Nguyen, T. Duong, O. Dobre, and O. Shin, "Joint information and jamming beamforming for secrecy rate maximization in cognitive radio networks," *IEEE Trans. Inf. Forensics Security*, vol. 11, no. 11, pp. 2609–2623, Nov. 2016.

[19] A. Garnaev, M. Baykal-Gursoy, and H. V. Poor, "A game theoretic analysis of secret and reliable communication with active and passive adversarial modes," *IEEE Trans. Wireless Commun.*, vol. 15, no. 3, pp. 2155–2163, Mar. 2016.
[20] Z. Cao, U. Tureli, and Y.-D. Yao, "User separation and frequency-time synchronization for the uplink of interleaved OFDMA," in *Proc. Conf. Rec. 36th Asilomar Conf. Signals Syst. Comput.*, vol. 2. Nov. 2002, pp. 1842–1846.
[21] S. Kay, *Fundamentals of Statistical Signal Processing: Detection Theory*. Englewood Cliffs, NJ, USA: Prentice-Hall, 1993.
[22] L. L. Scharf and B. Friedlander, "Matched subspace detectors," *IEEE Trans. Signal Process.*, vol. 42, no. 8, pp. 2146–2157, Aug. 1994.
[23] L. L. Scharf and M. L. McCloud, "Blind adaptation of zero forcing projections and oblique pseudo-inverses for subspace detection and estimation when interference dominates noise," *IEEE Trans. Signal Process.*, vol. 50, no. 12, pp. 2938–2946, Dec. 2002.
[24] R. T. Behrens and L. L. Scharf, "Signal processing applications of oblique projection operators," *IEEE Trans. Signal Process.*, vol. 42, no. 6, pp. 1413–1424, Jun. 1994.
[25] X. Zhang, *Matrix Analysis and Application*. Beijing, China: Tsinghua Univ. Press, 2004.
[26] C. Li and S. Roy, "Subspace-based blind channel estimation for OFDM by exploiting virtual carriers," *IEEE Trans. Wireless Commun.*, vol. 2, no. 1, pp. 141–150, Jan. 2003.
[27] *IEEE 802.22 Standard for Wireless Regional Area Networks Part 22: Cognitive Wireless RAN Medium Access Control (MAC) and Physical Layer (PHY) Specifications: Policies and Procedures for Operation in the TV Bands*, IEEE Standard 802.22, Jul. 2011.

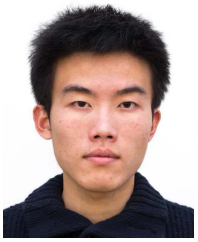

Huaxia Wang (S'13) received the B.Eng. degree in information engineering from Southeast University, Nanjing, China, in 2012. He is currently pursuing the Ph.D. degree with the Electrical and Computer Engineering Department, Stevens Institute of Technology, NJ, USA. In 2016, he was a Research Intern with the Mathematics of Networks and Systems Research Department, Nokia Bell Labs, Murray Hill, NJ, USA. His current research interests include wireless communications, cognitive radio networks, and machine learning.

Yu-Dong Yao (S'88–M'88–SM'94–F'11) received the B.Eng. and M.Eng. degrees from the Nanjing University of Posts and Telecommunications, Nanjing, in 1982 and 1985, respectively, and the Ph.D. degree from Southeast University, Nanjing, in 1988, all in electrical engineering. He was a visiting student with Carleton University, Ottawa, in 1987 and 1988.

He has been with the Stevens Institute of Technology, Hoboken, NJ, USA, since 2000, where he is currently a Professor and the Department Director of Electrical and Computer Engineering and also the Director of Stevens' Wireless Information Systems Engineering Laboratory. From 1989 to 2000, he was with Carleton University, Spar Aerospace Ltd., Montréal, and Qualcomm Inc., San Diego, CA, USA. He has been active in the nonprofit organization WOCC, Inc., which promotes wireless and optical communications research and technical exchange. He served as the WOCC President from 2008 to 2010 and the Chairman of the Board of Trustees from 2010 to 2012.

He holds one Chinese patent and 13 U.S. patents. His current research interests include wireless communications and networking, spread spectrum and CDMA, and cognitive radio. He was elected as an IEEE ComSoc Distinguished Lecturer from 2015 to 2016. In 2015, he was elected as a fellow of the National Academy of Inventors. He was an Associate Editor of the IEEE COMMUNICATIONS LETTERS from 2000 to 2008 and the IEEE TRANSACTIONS ON VEHICULAR TECHNOLOGY from 2001 to 2006, and an Editor of the IEEE TRANSACTIONS ON WIRELESS COMMUNICATIONS from 2001 to 2005.

Xin Zhang received the B.Eng. degree (Hons.) in electrical engineering from the University of Science and Technology Beijing, China, in 2008, and the M.Eng. degree in electrical engineering from the Beijing University of Posts and Telecommunications, China, in 2011. He is currently pursuing the Ph.D. degree in electrical engineering with the Stevens Institute of Technology, Hoboken, NJ, USA. He has been a Research and Teaching Assistant with the Department of Electrical and Computer Engineering, Stevens Institute of Technology, since 2013. His research interests include statistical signal processing, optimization algorithms, passive sensing, and multichannel signal processing.

Hongbin Li (M'99–SM'08) received the B.S. and M.S. degrees from the University of Electronic Science and Technology of China in 1991 and 1994, respectively, and the Ph.D. degree from the University of Florida, Gainesville, FL, USA, in 1999, all in electrical engineering.

From 1996 to 1999, he was a Research Assistant with the Department of Electrical and Computer Engineering, University of Florida. Since 1999, he has been with the Department of Electrical and Computer Engineering, Stevens Institute of Technology, Hoboken, NJ, USA, where he became a Professor in 2010. He was a visiting faculty member with the Air Force Research Laboratory in 2003, 2004, and 2009. His general research interests include statistical signal processing, wireless communications, and radars.

He has been a member of the IEEE SPS Signal Processing Theory and Methods Technical Committee (TC) and the IEEE SPS Sensor Array and Multichannel TC. He has been involved in various conference organization activities, including serving as a General Co-Chair for the seventh IEEE Sensor Array and Multichannel Signal Processing Workshop, Hoboken, June 17–20, 2012. He is a member of the Tau Beta Pi and Phi Kappa Phi. He has been an Associate Editor for *Signal Processing* (Elsevier), the IEEE TRANSACTIONS ON SIGNAL PROCESSING, the IEEE SIGNAL PROCESSING LETTERS, and the IEEE TRANSACTIONS ON WIRELESS COMMUNICATIONS, and a Guest Editor for the IEEE JOURNAL OF SELECTED TOPICS IN SIGNAL PROCESSING, and EURASIP *Journal on Applied Signal Processing*. He received the IEEE Jack Neubauer Memorial Award in 2013 from the IEEE Vehicular Technology Society, the Outstanding Paper Award from the IEEE AFICON Conference in 2011, the Harvey N. Davis Teaching Award in 2003 and the Jess H. Davis Memorial Award for excellence in research in 2001 from the Stevens Institute of Technology, and the Sigma Xi Graduate Research Award from the University of Florida in 1999.